Experimental Investigation and Analytical Study on the Flexural Behavior of Reinforced Recycled Aggregate Concrete Beams

George Wardeh and Elhem Ghorbel*

University of Cergy-Pontoise, 5 mail Gay LUSSAC, Neuville-sur-Oise 95031, France

Abstract: The paper presents an experimental study on the flexural behavior of reinforced beams made of natural and recycled gravels under monotonic loading. 20x25x170 cm beams specimens were prepared using two reinforcement ratios and were cast from two concrete mixtures. The two concretes are respectively a mixture of natural aggregates and a concrete with 100% recycled gravels of C35/45 strength class, S4 class of workability and a constant W/C ratio.

The results reported in this paper are those of experiments performed in the framework of this study beside 118 data sets taken from the literature on the flexural behavior of natural (NAC) and recycled aggregate concrete (RAC).

The principal results of bending tests show that flexural capacity of recycled aggregate concrete beams is similar to the flexural capacity of natural aggregate concrete beams for the service and ultimate loading. However, cracking moment, maximum crack spacing, crack heights and deflection under serviceable load are affected by the use of recycled aggregates.

Experimental results of the extensive data base were compared to load-carrying capacities and deflections calculated according to Eurocode 2 (EC2). The comparisons show that the method of deflection calculation does not correctly predict the experimental results.

Keywords: Recycled aggregates, reinforced concrete, flexural behavior, Eurocode2, equivalent replacement ratio.

1. INTRODUCTION

The number of concrete structures that complete their service life continues to rise and construction professionals are wondering about the future of concrete after the demolition. The use of recycled aggregates is one of the solutions able to reduce the environmental impact, the demand on land fill, as well as to conserve the natural resource. Therefore, numerous experimental studies have been conducted worldwide to analyze the properties of concrete with recycled aggregates [1-7]. Early research on the use of these aggregates have investigated their influence on the microstructure of concrete [1, 8] and on the mechanical properties as a function of replacement ratio [3-7, 9]. The researchers have concluded that it is possible to formulate concrete with recycled aggregates which have mechanical properties similar to those of concrete formulated with natural aggregates [6, 9]. Recent promising studies on the applicability of the recycled aggregates to reinforced concrete structural members have shown that Recycled Aggregate Concrete (RAC) can be used as a concrete structures [10-14]. Ajdukiewicz & Kliszczewicz [10] studied the performance of reinforced columns and beams, made with natural aggregates with those with 100% recycled gravels of the same class of compressive strength. They did not find any difference in the behavior of columns. However, they found that the bearing capacity of beams prepared with recycled concrete gravel decreased about 3.5% compared to the beams with natural aggregates. The reduction in ultimate strength is accompanied by an increase in the deflection.

Ignjatoviç *et al*, [12] found that, for identical compressive strength and reinforcement ratio, no difference between the behavior of natural aggregate and recycled aggregate concrete beams, regardless of the replacement ratio. However, the use of recycled aggregates greatly affects the crack maps and cracks sizes.

The present work deals with the flexural behavior of beams made with two concretes possessing the same workability and compressive strength. The first is formulated with natural aggregates; while the second is mixed with 100% recycled gravel obtained by recycling of a demolished building. In addition, a study on the applicability of EC2 [15] for the prediction of bearing capacity and the deflection has been made.

2. OBJECTIVE AND RESEARCH SIGNIFICANCE

This paper investigates the effect of the equivalent replacement ratio, which is taken equal to 1 when the granular skeleton is completely recycled, on the flexural behavior of RAC beams. By combining the experimental results of the present work with results available in the literature, the research incorporated

*Address correspondence to this author at the University of Cergy-Pontoise, 5 mail Gay LUSSAC, Neuville-sur-Oise 95031, France; Tel: +0033134256886; E-mail: elhem.ghorbel@u-cergy.fr

E-ISSN: 2409-9848/18 © 2018 Avanti Publishers

121 experimental data sets as the reference values, to evaluate the applicability of EC2 design equations to recycled aggregate concrete beams.

3. EXPERIMENTAL PROGRAM

3.1. Materials

CEM I CALCIA cement 52.5 N CE CP2 NF, manufactured in France and certified in conformity with the recommendations of standard EN 197-2 was used with a natural river sand (S 0.125-4 mm) and two types of gravels. The first is natural crushed (G1 4/10 and G2 10/20 mm), while the second is recycled. Recycled aggregates, resulting from demolition, were delivered in big bags and were sieved in laboratory into two classes: GR1 (4/10 mm) and GR2 (10/20 mm). The physical properties of natural and recycled aggregates are shown in Table **1**. From this table it can be seen that recycled aggregates are characterized by a lower density and higher water absorption capacity than natural ones. Finally, the used super plasticizer was Cimfluid 3002 with a solid content of 30%.

3.2. Concrete Mixtures

Two concretes were formulated in this work for the production of two sets of beams: a concrete with natural aggregates, considered as reference, NAC, and a concrete with 100% recycled coarse aggregates, named RAC100. NAC and RAC100 concrete mixtures were designed to have the same compressive strength of 35 MPa (class C35/45) and the same workability defined by a mean slump of 18±2 cm (S4 class of workability) workability according to the standard NF 206-1.

The reference concrete was formulated with a cement content of 360 kg/m^3 and a W/C equal to 0.5. The granular skeleton was optimized by the packing density's method. The optimal volumetric proportions of sand, S, gravel G1 and gravel G2 were taken such as $\frac{S}{G_1+G_2}=\frac{2}{3}$ and $\frac{G_1}{G_2}=1$. Finally, the super plasticizer dosage was adjusted experimentally to obtain a slump of 18 ± 2 cm using Abrams cone.

Table 1: Properties of Used Aggregates

	Sand	G1	G2	GR1	GR2
Density (kg/m^3)	2550	2510	2510	2240	2240
Water absorption. WA_{24} (%)	1.4	1.6	1.8	8.0	6.5

Deformed steel bars of diameters of 14 mm and 16 mm were used as the tensile reinforcement for this investigation. From the experimental data, the average yield strength was f_{yk}=550 MPa, the average elastic modulus was equal to Es=200 GPa, and the ultimate strain was ε_{uk} =10%. The stress-strain curve of steel bars is given in Figure **1**.

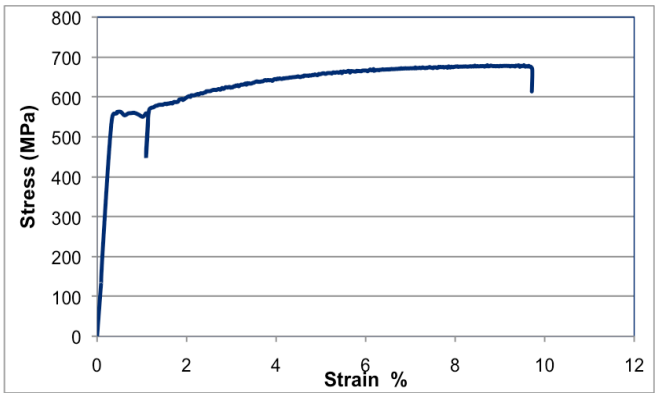

Figure 1: Stress-strain curve for a steel rebar of 12 mm.

For RAC100, the volume occupied by natural gravel was replaced by recycled ones, GR1 and GR2. Furthermore, an increase in natural sand content was necessary to achieve the optimal packing densities due to the low density of recycled gravels. The recycled gravel was considered dried and the amount of absorbed water was added to the mixing water. Furthermore, given the significant amount of water added to the mixing water, an additional quantity of cement was added such that the W/C ratio remains constant.

Finally mix proportions of two materials are given in Table **2** with fresh state properties. In this table, the effective water, E_{eff}, is taken equal to the total amount of water, E_{tot}, minus the water absorbed by recycled gravel (E_{eff} = E_{tot} - $WA_{24}xM_G$). It can be seen through the obtained results at fresh state that the materials satisfy the required workability. A decrease in density, accompanied by an increase in air content, when the replacement ratio increases can be also noticed. The

mix design method for these concretes is detailed in Wardeh *et al*, [6].

On the other hand, the concretes from literature were: 19 concretes from Sato *et al,* [14], 7 mixtures from Kang *et al*, [13], 4 concretes from Ignjatovic *et al*, [12] and 24 mixtures from Ajdukiewicz and Kliszczewicz [10]. The proportions of all mixes are given in Appendix A.

As the authors did not define the replacement ratio in the same way, a new equivalent substitution ratio, named r, is introduced in this work. This parameter is defined by the following expression:

$$r = \frac{V_{ra}}{V_{ra} + V_{na}} \quad \text{Eq. 1}$$

Hence, r = 1 when the sand and the gravel are entirely replaced by recycled aggregates. Based on this definition the equivalent ratio was recalculated for RAC100 (Table **2**) and for all selected concrete from the literature (Appendix A.).

3.3. Beam Specimens

Two beams with two longitudinal reinforcement ratios were made from each type of concrete (NAC and RAC100). The flexural reinforcement was 2HA14 and 2HA16 respectively (reinforcement ratios of 0.6% and

Table 2: Mix Proportions of Studied Materials

	NAC	RAC100
Cement (kg/m^3)	360	448
Effective water (W_{eff}) (kg/m^3)	180	180
Additional water (Wg) (kg/m^3)	-	53
Sand (kg/m^3)	703	930
Natural gravel G1 (kg/m^3)	346	-
Natural gravel G2 (kg/m^3)	692	-
Recycled gravel GR1 (kg/m^3)	-	218
Recycled gravel GR2 (kg/m^3)	-	326
Superplasticizer (l/m^3)	1.25	1.25
W_{eff}/C	0.50	0.40
W_{tot}/C	0.50	0.52
Paste volume (%)	29.6	37.8
Air content (%)	1.8±0.3	2.5±0.2
Slump (cm)	18±0.7	20 ±1.4
Equivalent replacement ration, r	0.00	0.40

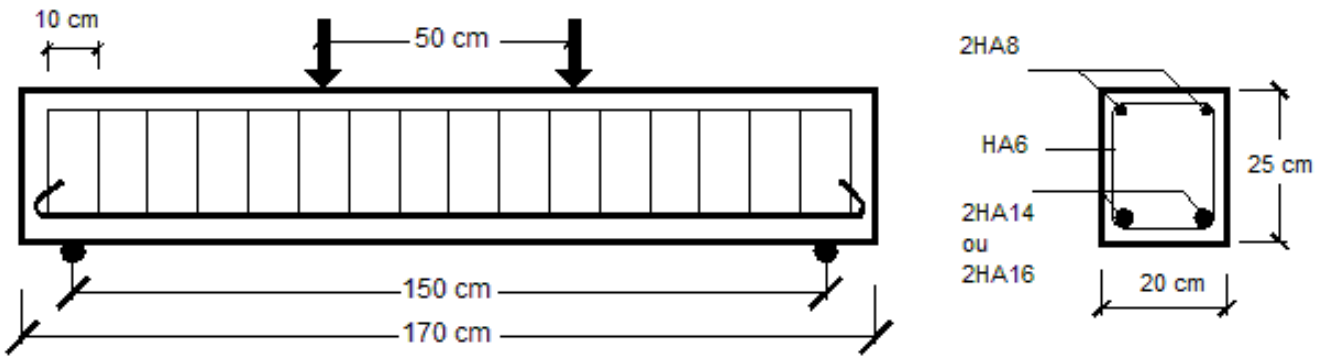

Figure 2: Details of tested beams.

Table 3: Properties of Hardened Concrete at 28 Days

	f_c (MPa)	f_t (MPa)	E (GPa)	Density (kg/m^3)	Porosity (%)
NAC	38,6±0.9	3,6±0.4	39,4±1.1	2250±67	12±0.79
RAC100	39,2±0.5	3,0±0.4	30,3±1.1	2043±22	20±0.77

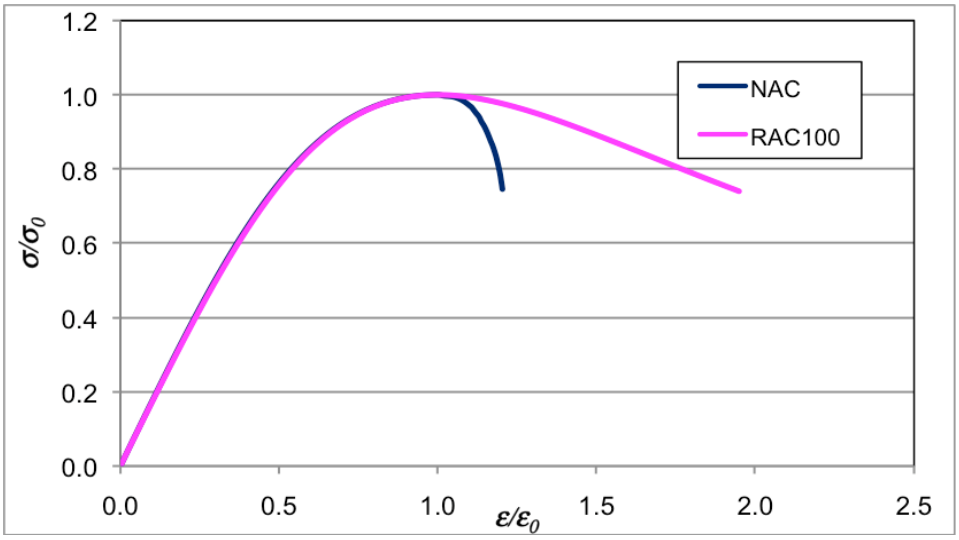

Figure 3: Stress-strain curves for tested concretes.

0.8% respectively). The shear reinforcement was made with deformed bars of 6mm diameter while the secondary reinforcement was ensured with bars of 8mm diameter. The details of this reinforcement for all beam specimens are shown in Figure **2**.

Additional 36 beams taken from the work of Sato *et al*, [14], 28 beams from Kang *et al*, [13], 9 beams from Ignjatovic *et al*, [12] and 48 beams from Ajdukiewicz and Kliszczewicz [10] were considered for the sake of comparison. The dimensions and the reinforcement details for these beams are given in Appendix B.

3.4. Instrumentation and Test Methods

All the beams were loaded up to failure using a 350-kN capacity hydraulic machine. The four-point bending tests were carried out under displacement control at a constant rate of 1 mm/min. Two concentrated loads were applied at 250 mm from mid-span at the top of the beams. The deflection was measured at the mid-span using a displacement transducer (LVDT) placed on the bottom of beam specimens. Other beams taken from the literature were tested under the same experimental conditions.

4. RESULTS AND DISCUSSION

4.1. Mechanical Properties of Concretes

The mechanical as well as the physical properties of studied concretes are summarized in table **3**. It can be observed that the strength class is achieved for both concretes while a decrease of tensile strength and elastic modulus is noticed. Moreover, the substitution of natural gravels by recycled ones induces a decrease in the density of the concrete and an increase in the porosity. This can be explained by the low density and high porosity of recycled aggregates [6].

These results are in agreement with those of the literature as shown in Appendix B[10, 12-14]. Figure **3** shows stress–strain curves for NAC and RAC100 concretes respectively. From the obtained curves, it can be seen that the shape of the descending branch is more spread when recycled gravels are used. This observation highlights a more dissipative behavior when recycled aggregates are used, and may be explained by a more diffuse damage related to the nature of recycled aggregates [6].

4.2. Flexural Behavior and Cracking Patterns

Load-mid-span deflection relationships obtained from the tests are illustrated in figure **4**. Each curve

consists of three lines with different slopes. The deflections corresponding to the cracking load F_{cr}, yielding load F_y, and ultimate load $F_u$are defined as cracking deflection Δ_{cr}, yielding deflection Δ_y and ultimate deflection Δ_u (Figure **4**).

From the tests, it is shown that the NAC beams have larger stiffness and slightly higher bearing capacity than those of the RAC100 beams. The loss of stiffness can be explained by the decrease of the elastic modulus and the more pronounced cracked state of RAC whatever the reinforcement ratio. All important results are recapitulated in table **4**. It can be shown that the results are almost identical for the two concretes despite the slight decrease in the cracking moment which is due to the decrease of tensile strength of RAC.

The observed failure mode of beams is related to the steel yielding whatever the reinforcement ratio. Concrete crushing occurred after the yielding of the steel under load points. By the end of the test, inclined

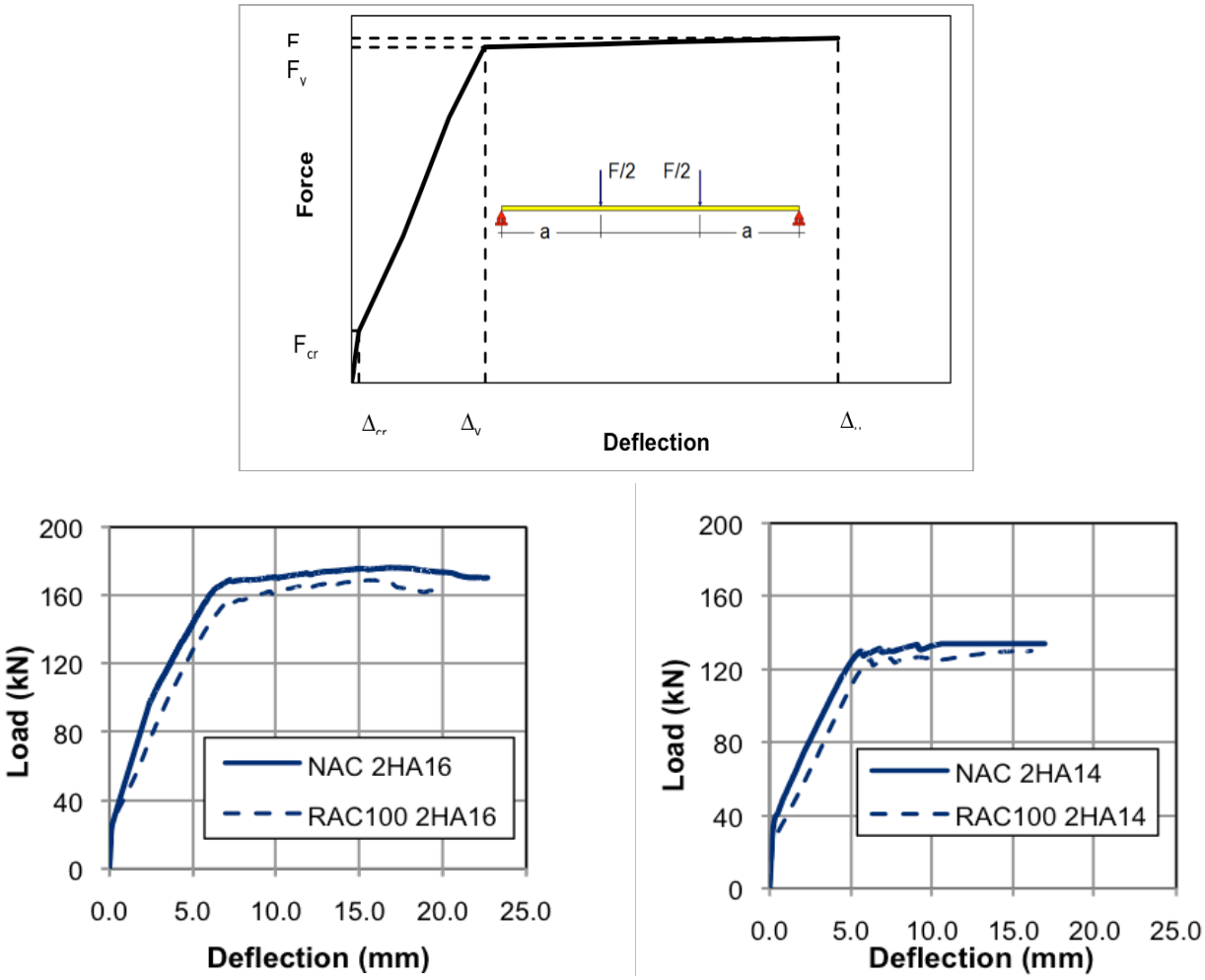

Figure 4: Load–deflection curves of concretes for different reinforcement ratios.

Table 4: Summary of Test Results

Test ID	r	Mcr* (kN.m)	My** (kN.m)	Mu*** (kN.m)	Δ_{cr} (mm)	Δ_y (mm)	Δ_u (mm)
NAC2HA14	0,00	8.0	42.3	44.0	0.2	7.0	21.0
RAC1002HA14	0.40	6.9	39.5	42.2	0.2	7.3	20.2
NAC2HA16	0.00	8.0	32.0	33.5	0.2	6.0	17.0
RAC1002HA16	0.40	6.7	31.4	32.5	0.2	6.2	16.2
*$M_{cr}=F_{cr}.a/2$,** $M_y=F_y.a/2$, *** $M_u=F_u.a/2$.							

Table 5: Cracking Details of Studied Beams

Author	Test ID	r	ρ (%)	Number of Cracks	Cracked Area's width (cm)	Cracks Mean Spacing (cm)	Means Height (cm)
Present work	NAC 2HA14	0.0	0.6	12	125	11.0	17.0
	RAC100 2HA14	0.4	0.6	15	130	7.0	20.0
	NAC 2HA16	0.0	0.8	11	120	11.0	17.0
	RAC100 2HA16	0.4	0.8	12	120	10.0	18.0
Ajdukiewicz & Kliszczewicz [10]	BNNh-b1	0.0	0.8	31	174	6.0	25.0
	BRNh-b1	0.7	0.8	34	198	5.6	26.5
	BRRh-b1	1.0	0.8	39	207	5.0	26.5
	BNNh-b2	0.0	1.3	35	197	6.5	24.4
	BRNh-b2	0.7	1.3	37	228	5.6	25.7
	BRRh-b2	1.0	1.3	40	230	5.3	26.9
Sato *et al,* [14]	v-01-13DB	0.0	0.9	23	148	8.7	15.5
	CFR-01-13DB	1.0	0.9	23	202	11.9	16.7
	HV-01-13DB	0.0	0.9	29	176	9	17.5
	HCFR-01-13DB	1.0	0.9	37	209	8	17.8

cracks, due to the shear force, appeared near supports. All cracks patterns appeared at lower loads for RAC100 beams compared to NAC beams. Moreover, it can be noticed that the number of cracks increases when recycled gravels are used. This cracked state is accompanied by a decrease in the spacing between cracks and an increase in the width of the cracked zone and finally an increase in the height of the cracks (Table **5**). As shown in the table, the same conclusion can be generalized to the beams of the literature where it is clear that the situation is more pronounced when the replacement ratio is higher. RAC beams exhibited a wide range of cracks that more spread out than NAC beams [10-14].

Figure **5** represents the evolution of the number of cracks as a function of the incrementally applied load. It is clearly visible that when the load level is low, the influence of recycled aggregates is not significant. For higher loads the number of cracks increases quickly for RAC100 beams. According to Kang *et al,* [13] this phenomenon is due to a loss of bond strength between RAC concrete and reinforcing steel. The evolution of the number of cracks depending on load can be modeled by the following equation:

$$N_{cr} = \alpha\left(F - F_{cr}\right) \qquad \text{Eq.1}$$

In figure **5**, equation 2 is plotted for all tested beams. It seems the slope, α, depends on both the nature of concrete and the reinforcement ratio. This slope is important for RAC beams and its value increases when the reinforcement ratio is low.

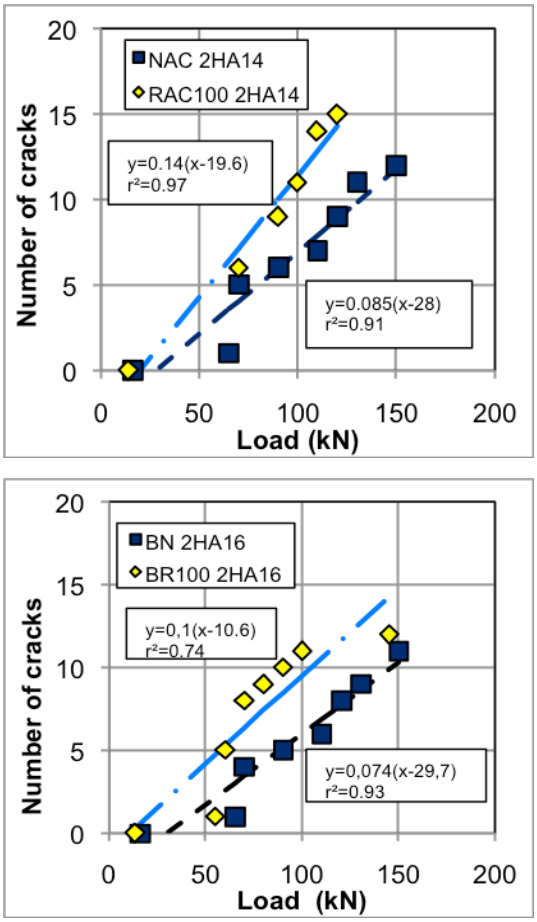

Figure 5: Evolution of the number of cracks.

4.3. Comparative Analysis of Results

In order to investigate the effect of the equivalent replacement ratio on the flexural behavior of RAC beams, the experimental results from the current study were compared with the test data available in the literature for RAC beams[10, 12-14](Appendix C). The results for a total of 122 beam test data are plotted in figures **6-8**. In these figures the ratios of bending moment of RAC beams and bending moment of control NAC beams are presented as a function of the equivalent replacement ratio.

Form Figure **6** it can be noticed that the cracking moment of RAC beams is equal or lesser when compared to the cracking moment of corresponding NAC beams (r=0) except four beams from Sato and two from Ajdukiewicz. The decrease in cracking moment is due mainly to the decrease in the tensile strength of concrete. For these beams, the difference could be due to an underestimation of the tensile strength.

The yielding moment, M_y, for RAC beams is practically the same for NAC beams. The mean ratio M_y/M_{y0} for all data points is 1.0 with a standard deviation of 4% (Figure **7**). Among the 122 beams, only 23 beams showed an increase in M_y. These beams are respectively 7 of Sato *et al,* [14], 1 of Ignjatoviç *et al,* [12], 9 of Kang *et al,* [13], and finally 6 of Ajdukiewicz & Kliszczewicz[10].

In addition, 18 RAC beams had a yielding moment between 90 and 95% of NAC control beams. These

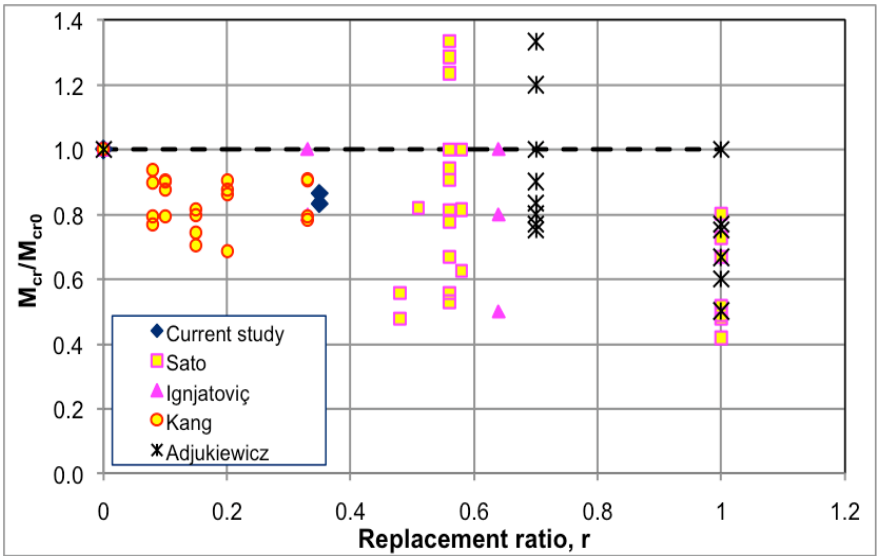

Figure 6: Influence of the recycled aggregates percentage on the critical moment of cracking.

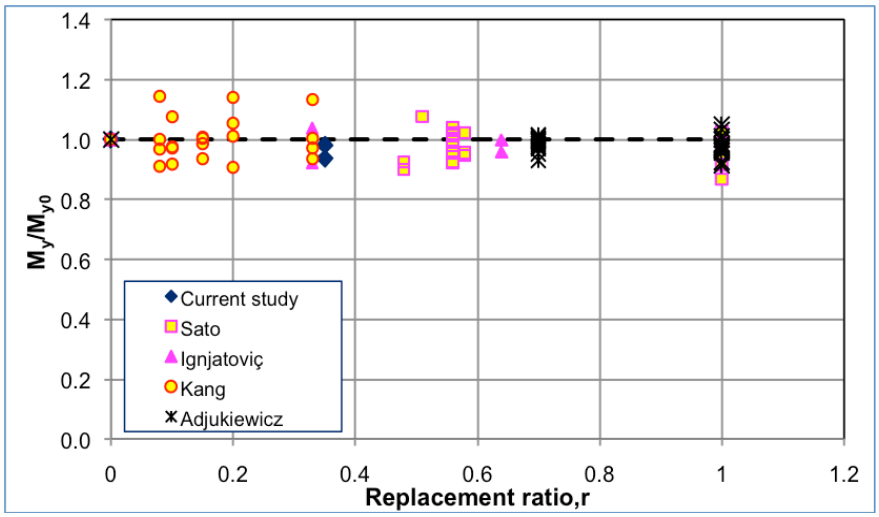

Figure 7: Influence of the recycled aggregate percentage on the yielding moment.

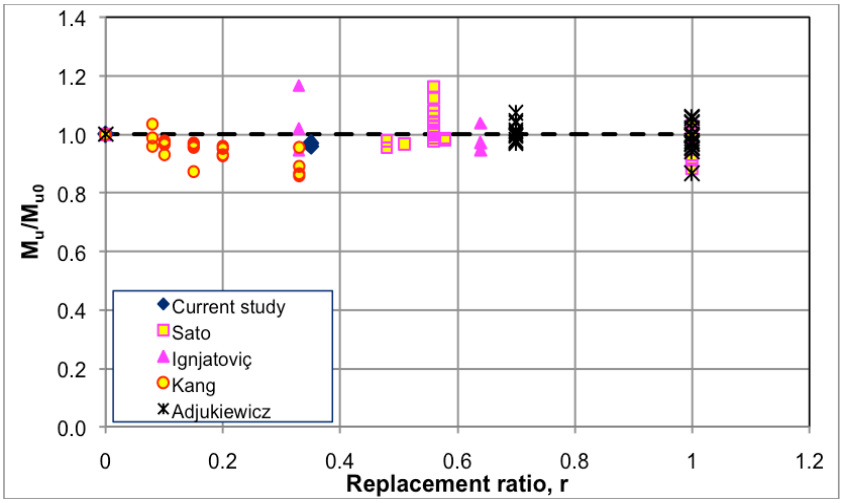

Figure 8: Influence of the recycled aggregate percentage on the ultimate moment.

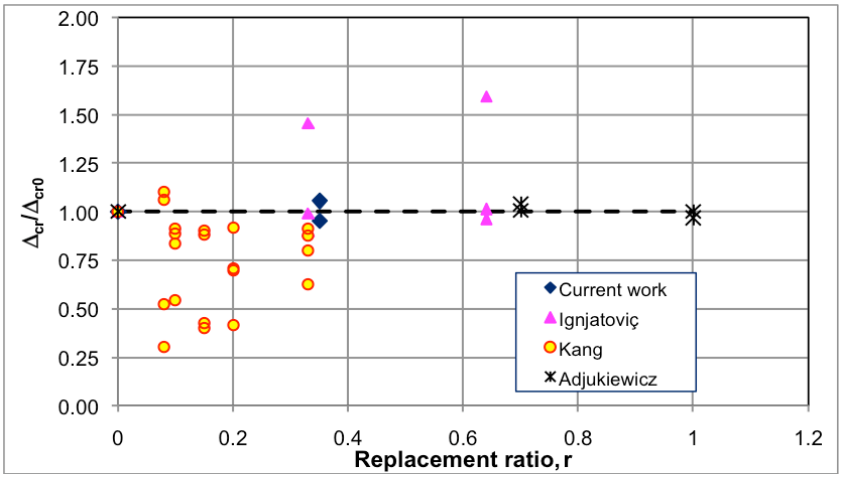

Figure 9: Influence of the recycled aggregate percentage on the critical deflection.

beams are respectively, 1 of the current study (RAC100 2HA16), 8 of Sato *et al*, [14], 1 of Ignjatoviç *et al*, [12], 5 of Kang *et al,* [13]and 3 of Ajdukiewicz & Kliszczewicz [10]. Finally only one beam from Sato *et al*, [14] had a moment less than 90% of the NAC control beam.

The small scattering of results, whatever the replacement ratio, can be explained by the fact that the average ratio between RAC and NAC compressive strength obtained from analyzed data was 0.93 with a standard deviation of 11%.

The average value of the ratio M_u/M_{u0} for all data points is 0.99 with a standard deviation of 5% (Figure **8**). Based on the test data, only 28 RAC beams showed a larger ultimate failure moment, Mu, than the control NAC beams. These beams are respectively, 11 of Sato *et al*, [14], 3 of Ignjatoviç *et al*, [12] and 12 of Ajdukiewicz & Kliszczewicz [10]. Moreover 13 showed an ultimate moment less than the control NAC beams. There are 3 beams of Sato *et al*, 1 of Ignjatoviç *et al*, 7 of Kang *et al,* and finally 2 Ajdukiewicz & Kliszczewicz.

The ratios of RAC beams deflections and that of control NAC beams are plotted in Figures **9-11**. As shown in Figure **9**, the deflection related to the critical load decreases in general as the critical moment decreases with exception for few beams of Ignjatoviç *et al*. For these beams the deflection was higher than the deflection of the control NAC beams.

In Figure **10** it can be shown that the RAC beams deflections are in general higher than the control NAC beams. The average value of the ratio Δ_y/Δ_{y0} for all data points is 1.04 with a standard deviation of 7.5%. This slight increase can be explained by the degradation of RAC flexural stiffness due to the reduced modulus of elasticity, the crack pattern, and the bond deterioration [11-13].

The measured beams deflections at failure loads are in general lower for RAC beams than for the control NAC beams (Figure **11**). This deflection reflects the change in the ultimate bending moment, M_u, (Figure **8**) and the compressive strength of the concrete for the same reinforcement ratio. When this latter decreases, the deflection decreases whatever the replacement ratio and the reinforcement ratio.

The most important decrease was observed for the normal strength concrete beams (series N) of Kang *et al*, [13].The ratio between the compressive strength of RAC and the compressive strength of control NAC beams is equal to 0.8 with a standard deviation of 5% and the mean ratio between failure moments is 0.95 with a standard deviation of 5.5%.

Twelve RAC beams of Sato *et al*, [14] have shown a deflection at failure lower than0.95 of the corresponding NAC beams. The failure deflections of beams cr60-01-13db, cfr45-03-wb, cfr60-03-wb, cfrex45-03-wb made with 100% recycled aggregates are 12%, 18 %, 41%, 39% lower than those of NAC beams respectively. The ratios between RAC and NAC failure moments were 0.99, 0.91, 0.89 and 0.88. The failure deflections of beamsfr60-01-13wb, fr60-01-13dbwith 100% recycled sand are 11% and 19% lower than the corresponding NAC beams. The ratios between RAC and NAC failure moments for these beams were 0.98, 0.94 respectively while the ratios of compressive strengths were 0.8 and 0.73. The other beams which showed a drop in the failure deflection are mainly from the two mixes cr45 and cr60. The average ratios between RAC and NAC deflections was 0.85 with a standard deviation of 11% corresponding to a mean ratio of compressive strength of 0.85 too with a standard deviation of 10%.

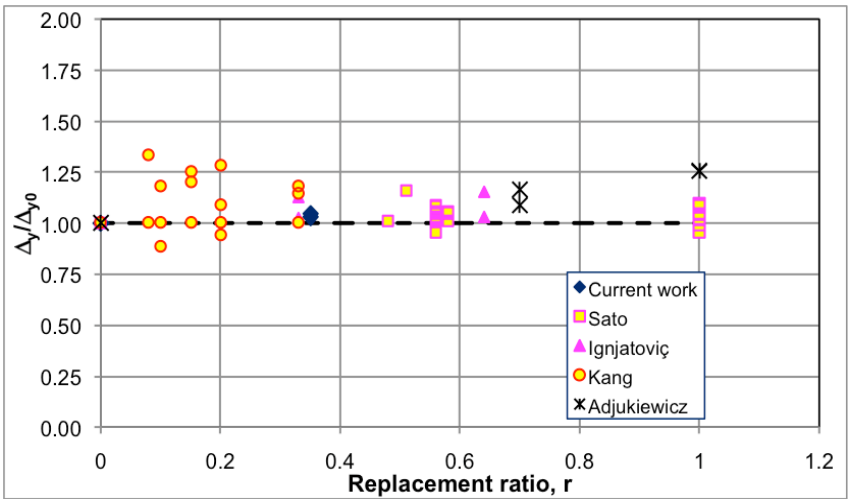

Figure 10: Influence of the recycled aggregate percentage on the yielding deflection.

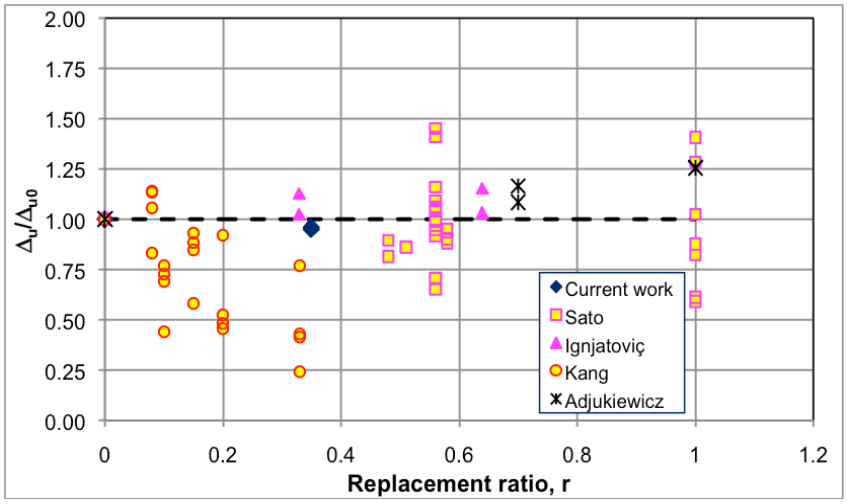

Figure 11: Influence of the recycled aggregate percentage on the ultimate deflection.

5. MODELING OF LOAD-DEFLECTION CURVE ACCORDING TO EC2

The analysis of a section subjected to pure bending is based on the following assumptions:

- Strain distribution is assumed to be linear and the strain at any point is proportional to the distance from the neutral axis.
- The strain in the reinforcement is equal to the strain in the concrete at the same level.
- The stresses in the concrete and steel may be calculated using the simplified stress-strain relationships.
- The contribution of concrete in tension is neglected.
- To simplify the calculation of concrete compression force, an equivalent rectangular stress block may be used.

The above assumptions are sufficient to calculate the resultant forces developed by the section to balance the applied loads.

5.1. Stress-Strain Relationships

The stress-strain diagram for concrete subjected to axial compression is shown in figure **12**. This diagram is defined as follows [15]:

$$\sigma_c = \begin{cases} f_{cd}\left[1-\left(1-\dfrac{\varepsilon_c}{\varepsilon_{c2}}\right)^n\right] & 0 \le \varepsilon_c \le \varepsilon_{c2} \\ f_{cd} & \varepsilon_{c2} \le \varepsilon_c \le \varepsilon_{cu2} \end{cases} \quad \text{Eq.2}$$

$$n = \begin{cases} 2 & f_c^{'} < 50 \ \ MPa \\ 1.4 + 23.4\left[\dfrac{90 - f_c^{'}}{100}\right]^4 & f_c^{'} \ge 50 \ \ MPa \end{cases} \quad \text{Eq.3}$$

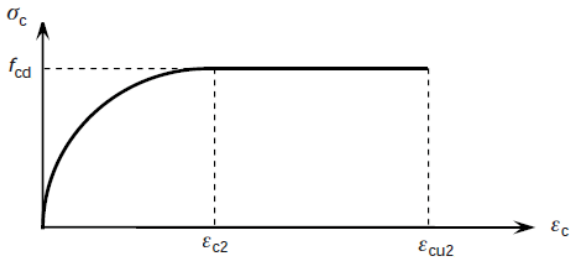

Figure 12: Idealized stress-strain curve for concrete.

The ultimate strain of concrete, ε_{cu2}, is given by the following expressions:

$$\varepsilon_{cu2}(‰) = \begin{cases} 3.5 & f_c^{'} \le 50 \ \ MPa \\ 2.6 + 35\left(\dfrac{90 - f_c^{'}}{100}\right)^4 & f_c^{'} > 50 \ \ MPa \end{cases} \quad \text{Eq.4}$$

Other simplified diagrams are admitted as the rectangular diagram shown on figure **13**. η and λ are reduction factors taken as:

$$\begin{cases} \eta = 1.0 \\ \lambda = 0.8 \end{cases} \quad f_c^{'} \le 50 \ \ MPa \quad \text{Eq.5}$$

$$\begin{cases} \eta = 1 - \dfrac{(f_c^{'} - 50)}{200} \\ \\ \lambda = 0.8 - \dfrac{(f_c^{'} - 50)}{400} \end{cases} \quad 50 < f_c^{'} \le 90 \ \ MPa \quad \text{Eq.6}$$

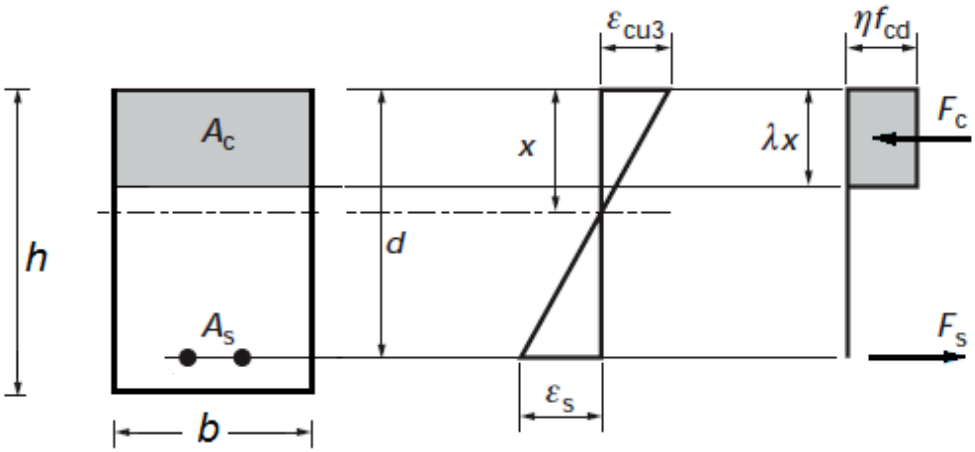

Figure 13: Behavior of reinforced concrete beam section at the ultimate limit states.

The stress-strain diagram for steels according to Eurocode 2 [15] is represented in the figure **14**. For normal design, either of the following assumptions may be made:

- An inclined top branch with a strain limit of ε_{ud} and a maximum stress of $k\frac{f_{yk}}{\gamma_s}$ where $k=\left(\frac{f_t}{f_y}\right)_k$. The value of k is between 1.15 and 1.35.
- A horizontal top branch without the need to check the strain limit.

The recommended value ofε_{ud} is 0.9 ε_{uk}. The value of ε_{uk} depends on the class of ductility and it is limited to 2.5% for class A, 5% for class B and 7.5% for class C.

5.2. Singly Reinforced Rectangular Section in Bending

Before craacking, it is assumed that both the concrete and the reinforcement behave elastically. Assuming a linear variation of the strain over the cross-section, the stress distribution is obtained by the classical beam theory. When the tensile strength is reached at the tensile side of the beam the concrete is assumed to crack and the formed crack extends to the level of the neutral axis. The cracking bending moment is expressed by the following equation:

$$M_{cr}=\frac{f_t I_g}{d-x} \qquad \text{Eq.7}$$

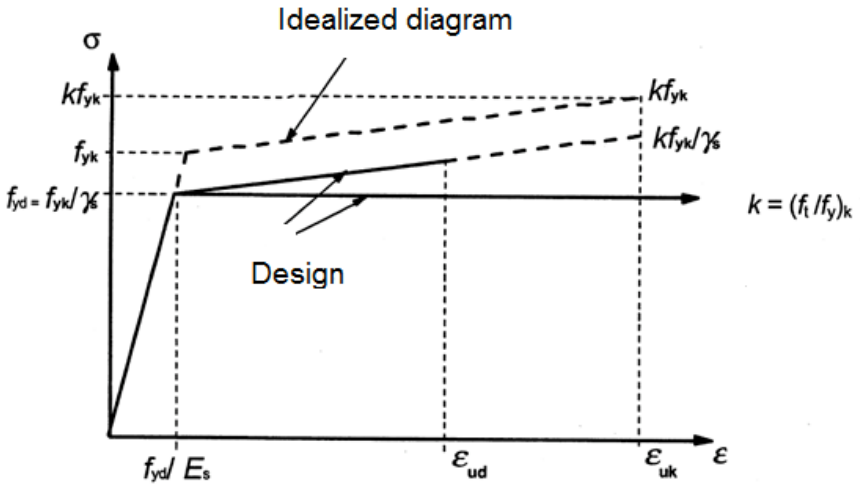

Figure 14: Design stress-strain diagrams for reinforcing steel according to Eurocode 2.

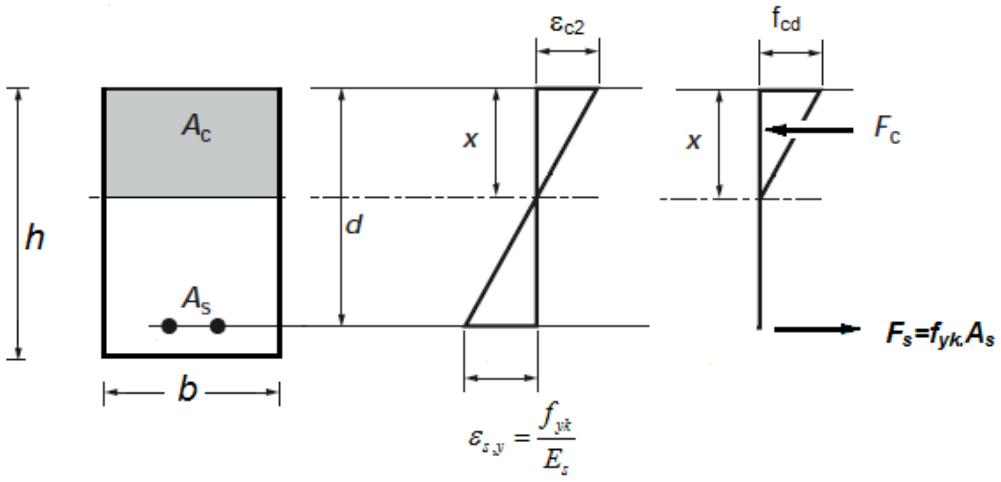

Figure 15: Behavior of reinforced concrete beam section with flexure at first yield.

In reinforced concrete sections, the yielding moment M_y, is reached when the tension reinforcement first reaches the yield strength, f_{yk}. It is well accepted that the distribution of stresses stills linear over the cross section at the yielding stage [16, 17] (figure **15**). The static equilibrium equation of the internal forces applied on the section can be written as;

$$\frac{1}{2} f_{cd}.b.x = A_s.f_{yk} \quad \text{Eq.8}$$

The yield bending moment is expressed by the following equation:

$$M_y = A_s.f_{yk}\left(d - \frac{x}{2}\right) \quad \text{Eq.9}$$

Referring to figure **13**, the equilibrium at the ultimate limit state is expressed by the following equation:

$$A_s.f_{yk} = \lambda x b \eta f_{cd} \quad \text{Eq.10}$$

Consequently the ultimate bending moment is given by:

$$M_u = \lambda x b \eta f_{cd}\left(d - \frac{\lambda x}{2}\right) \quad \text{Eq.11}$$

5.3. Calculation of Deflection

The method proposed by EC2 part 7.3.2 [15] is used to calculate the deflection of all beams. According to this method, a reinforced concrete member is divided into fully cracked and uncracked regions. In the uncracked region both the concrete and steel behave elastically, while reinforcing steel carries all the tensile force on the member after cracking. The deflection of the member is obtained by the double integration of the mean curvature, which is expressed as:

$$\frac{1}{r} = \zeta\left(\frac{1}{r}\right)_{cr} + (1-\zeta)\left(\frac{1}{r}\right)_{nc} \quad \text{Eq.12}$$

By using double integration of curvatures, the deflection can then be obtained.

6. COMPARISON BETWEEN EXPERIMENTAL RESULTS AND EC2 PREDICTIONS

The bending moments were calculated according to EC2 as explained in paragraph 5. The results for the 122 beam test data are plotted in figures **16** to **18**. It can be observed that the results of the experimental studies are very close to the predicted results except for the cracking moment (Figure **16**). For the latter, the farthest results were essentially for concretes taken form Ignjatoviç *et al*, [12] and of Ajdukiewicz & Kliszczewicz [10]. In addition, four beams of Kang *et al*, [13] gave predicted cracking moments lower than the experimental ones. They are respectively N0-1.8, N15-1.8, N30-1.8 and N50-1.8 whence the problem is related to the reinforcement ratio and not the recycled aggregates. The correlation ratio for the identity line is r^2=0.66.

For yielding and failure moments, the identity line fits the data points with correlation ratio of r^2=0.99 and r^2=0.95 respectively. From figure **18** it can be observed that the failure moment of two points of Ignjatoviç *et al*, [12] are clearly far from the identity line X=Y. They are RAC50-3 and RAC100-3 where the reinforcement ratio

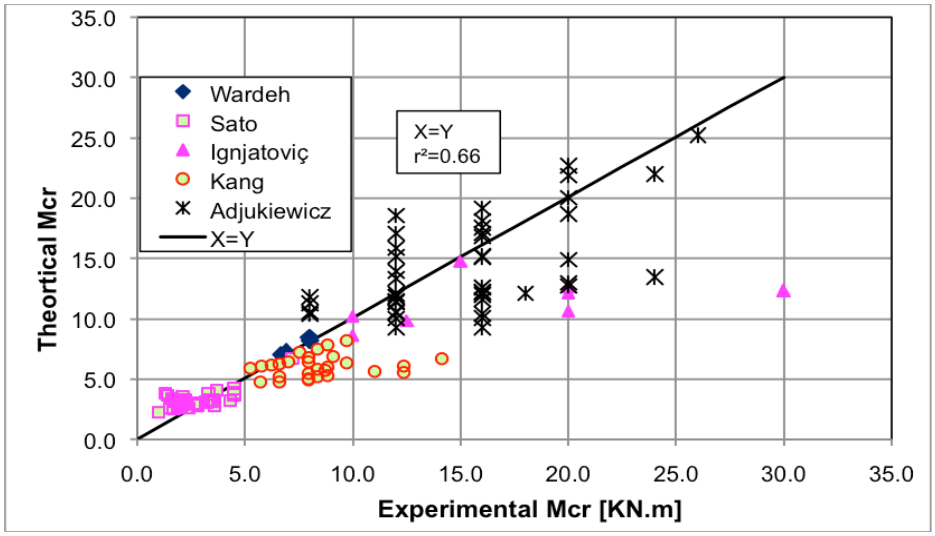

Figure 16: Comparison of test results and analytical predictions for cracking moment.

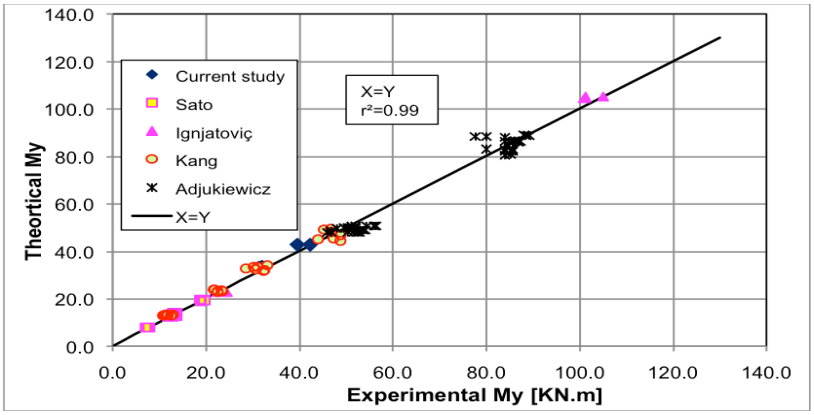

Figure 17: Comparison of test results and analytical predictions for yielding moment.

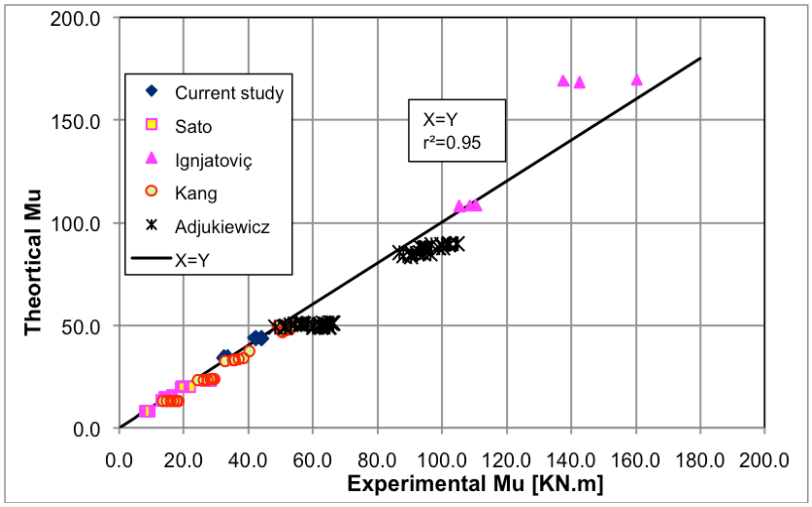

Figure 18: Comparison of test results and analytical predictions for failure moment.

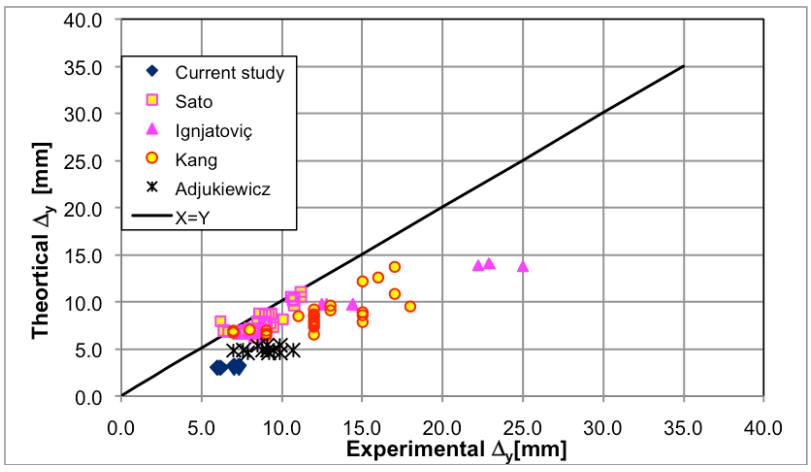

Figure 19: Comparison between experimental and predicted yielding deflection.

is 2.12%. Hence, the difference is due to the high reinforcement ratio and not to recycled aggregates.

The mid-span deflection was calculated for all studied beams according to EC2 following the method explained in paragraph 5. Comparing the experimental values with theoretical predictions, it can be observed that for the yielding deflection, the EC2approach compares reasonably well with the experimental data (Figure **19**).

A significant difference was observed, however, for both cracking and ultimate deflections. For ultimate deflection, EC2 procedure takes no account of two effects, namely deformation due to bond-slip of longitudinal bars and shear deformation due to the formation of diagonal cracks.

7. CONCLUDING REMARKS

The paper investigated the flexural behavior of reinforced recycled concrete beams. Four beam specimens from natural and 100% recycled gravel concretes, with two different reinforcing bar ratios, were tested. Both concretes were formulated to have the same compressive strength and workability.

From the test results and calculated values, the following conclusions are drawn:

- At the same compressive strength, Recycled aggregate concretes had lower elastic modulus, splitting and flexural tensile strength than normal aggregate.
- The flexural capacity does not decrease by using recycled aggregates. However, the deflection is affected by the use of recycled aggregates. When the replacement ratio increases, the cracking and failure deflections decrease while the yielding deflection increases.
- RAC beams showed a greater number of cracks, a lower cracking moment and an increase in the width of the cracked zone. These observations are similar to remarks of previous studies found in the literature.

Test results of the present study with the results of 118 beams found in the literature show that EC2 is adequate for the calculation of the flexural capacity of RAC beams. However, the prediction of deflections using EC2 underestimates beams deflections.

NOTATIONS

As Cross-sectional area of tension steel reinforcement,

b Width of rectangular crosses section,

h Beam height,

d Depth of centroid of tensile steel reinforcement from extreme compression fiber,

E Elastic modulus of concrete,

Es Elastic modulus of steel,

f'c Compressive strength of concrete,

fcd The maximum design compressive strength,

ft Tensile strength of concrete,

fyk Yield strength of steel,

L Span length,

M_{cr} The bending moments on the cross-section at first cracking,

M_y The bending moments on the cross-section at steel yielding,

M_u The ultimate flexural capacity,

M Applied bending moment,

n Exponent taken into account the class of concrete,

Δ_{cr} Deflection at cracking,

Δy Deflection at yielding,

Δu Ultimate deflection,

1/r Average curvature,

$1/r_{cr}$ Curvature calculated for fully cracked section,

$1/r_{uc}$ Curvature calculated for uncracked section,

ε_{c2} The strain related to the maximum compressive strength fcd,

ε_{cu} The ultimate strain of concrete,

$\varepsilon_{y,d}$ The elastic strain of steel rebar,

ε_{uk} The ultimate strain of steel rebar,

ε_{ud} The recommended design value of steel rebar$\varepsilon_{ud}=0.9\varepsilon_{uk}$,

σ_c Stress in concrete,

β Load duration factor (1 for single short-term loads; 0.5 for sustained loads),

ξ Coefficient given by $\xi = 1 - \beta\left(\frac{M_{cr}}{M}\right)^2$,

I_g The moment of inertia of the uncracked section,

x The distance from the neutral axis to the extreme fiber in compression,

V_{na} Volume of natural aggregates (m^3),

V_{ra} Volume of recycled aggregates (m^3),

r Equivalent replacement ratio,

ρ Reinforcement ratio,

N_{cr} Number of cracks,

α Correlation coefficient.

APPENDIX A. MIX DESIGN OF STUDIED CONCRETE

Table A.1: Mixture Proportions of Beams Taken from Sato *et al*, [14]

Mix	Cement (kg/m^3)	Water (kg/m^3)	Natural Aggregates		Recycled Aggregates		W/C	Paste volume (m^3/m^3)	Replacement Ratio r (-)
			Sand (kg/m^3)	Gravel (kg/m^3)	Sand (kg/m^3)	Gravel (kg/m^3)			
V-01	283	170	860	900	-	-	0.60	0.26	0.00
CR45-01	278	167	872	-	-	900	0.60	0.26	0.56
CR60-01	278	167	872	-	-	900	0.60	0.26	0.56
FR60-01	308	185	-	948	732	-	0.60	0.28	0.47
CFR-01	293	176	-	-	755	855	0.60	0.27	1.00
HV-01	645	161	656	996	-	-	0.25	0.37	0.00
HCFR-01	645	161	-	-	581	902	0.25	0.37	1.00
V30-03	593	178	647	932	-	-	0.30	0.37	0.00
CR30-03	593	178	648	-	-	853	0.30	0.37	0.58
CFR30-03	588	177	-	-	543	870	0.30	0.37	1.00
V45-03	381	171	727	1048	-	-	0.45	0.29	0.00
CR45-03	381	171	727	-	-	958	0.45	0.29	0.58
CFR45-03	378	170	-	-	625	960	0.45	0.29	1.00
V60-03	311	187	840	935	-	-	0.60	0.29	0.00
CR60-03	292	164	859	-	-	848	0.56	0.26	0.51
CFR60-03	309	186	-	-	706	886	0.60	0.29	1.00
VEX45-03	351	171	727	1048	-	-	0.49	0.28	0.00
CREX45-04	351	171	625	-	-	958	0.49	0.28	0.58
CFREX45-05	348	170	-	-	625	960	0.49	0.28	1.00

Table A.2: Mixture Proportions of Beams Taken from Kang *et al*, [13]

Mix	Cement (kg/m^3)	Water (kg/m^3)	Silica fume (kg/m^3)	Sand (kg/m^3)	Coarse gravel		W/C	Paste volume (m^3/m^3)	Replacement Ratio r (-)
					Natural (kg/m^3)	Recycled (kg/m^3)			
H0	350	122.5	150	870	662.3	-	0.35	0.29	0.00
H15	350	122.5	150	870	563	99.4	0.35	0.29	0.08
H30	350	122.5	150	870	463.6	198.7	0.35	0.29	0.15
N0	365	164.3	-	743	975	-	0.45	0.28	0.00
N15	365	164.3	-	743	828.8	146.3	0.45	0.28	0.10
N30	365	164.3	-	743	682.5	292.5	0.45	0.28	0.20
N50	365	164.3	-	743	487.5	487.5	0.45	0.28	0.33

Table A.3: Mixture Proportions of Beams Taken from Ignjatovic [12]

Mix	Cement (kg/m^3)	Water (kg/m^3)	Sand (kg/m^3)	Natural gravel (kg/m^3)	Recycled gravel (kg/m^3)	W/C	Paste volume (m^3/m^3)	Replacement ratio r (-)
NAC	354	185	600	1164	-	0.52	0.30	0.00
RAC50	354	205	598	555	555	0.58	0.32	0.33
RAC100	365	234	576	0	1071	0.64	0.35	0.64

Table A.4: Mixture Proportions of Beams Taken from Ajdukiewicz and Kliszczewicz [10]

Mix	Cement (kg/m^3)	Water (kg/m^3)	Silica fume (kg/m^3)	Sand (kg/m^3)	Natural gravel (kg/m^3)	Recycled Aggregates		W/C	Paste volume (m^3/m^3)	Replacement ratio r (-)
						Sand (kg/m^3)	Gravel (kg/m^3)			
ONNl	300	148	-	607	1416	-	-	0.49	0.24	0.00
ORNl	300	181	-	549	-	-	1281	0.60	0.28	0.70
ORRl	300	224	-	-	-	530	1236	0.75	0.32	1.00
ONNm	500	180	-	523	1222	-	-	0.36	0.34	0.00
ORNm	500	192	-	480	-	-	1119	0.38	0.35	0.70
ORRm	500	218	-	-	-	462	1079	0.44	0.38	1.00
GNNl	300	148	-	600	1400	-	-	0.49	0.25	0.00
GRNl	300	169	-	563	-	-	1312	0.59	0.27	0.70
GRRl	300	214	-	-	-	548	1279	0.71	0.31	1.00
GNNm	500	180	-	524	1255	-	-	0.36	0.34	0.00
GRNm	500	180	-	491	-	-	1312	0.36	0.34	0.70
GRRm	500	207	-	-	-	548	1279	0.41	0.37	1.00
GNNh	455	126	45	551	1286	-	-	0.28	0.29	0.00
GRNh	455	126	45	517	-	-	1205	0.28	0.29	0.70
GRRh	455	133	45	-	-	503	1175	0.29	0.30	1.00
BNNl	300	148	-	654	1524	-	-	0.49	0.24	0.00
BRNl	300	148	-	582	-	-	1358	0.49	0.24	0.70
BRRl	300	178	-	-	-	575	1342	0.59	0.27	1.00
BNNm	500	180	-	570	1330	-	-	0.36	0.34	0.00
BRNm	500	194	-	510	-	-	1188	0.39	0.36	0.70
BRRm	500	214	-	-	-	503	1174	0.43	0.38	1.00
BNNh	500	108	45	620	1447	-	-	0.22	0.29	0.00
BRNh	500	108	45	554	-	-	1292	0.22	0.29	0.70
BRRh	500	121	45	-	-	547	1276	0.24	0.30	1.00

APPENDIX B. MECHANICAL PROPERTIES OF STUDIED CONCRETES

Table B.1: Characteristics of Beams Studied from the Experimental Program of Sato *et al*, [14]

Test ID	Curing	Age (day)	Span (m)	Section		As (mm^2)	ρ (%)	f'c (MPa)	ft (MPa)	E (MPa)	fyk (MPa)
				b(m)	h(m)						
v-01-10WB	wet	65	2.2	0.15	0.20	157.1	0.5	30.60	2.9	30324	332
v-01-10WB	dry	121						32.50	3.0	29200	
cr45-01-10wb	wet	57						30.40	2.6	20000	
cr45-01-10db	dry	108						28.40	2.4	24975	
cr60-01-10wb	wet	142						34.5	2.8	22635	
cr60-01-10db	dry	134						31.8	3.3	23950	
v-01-13WB	wet	65				265.5	0.9	30.60	2.9	30324	353
v-01-13WB	dry	121						32.50	3.0	29200	
cr45-01-13wb	wet	57						30.40	2.6	20000	
cr45-01-13db	dry	108						28.40	2.4	24975	
cr60-01-13wb	wet	142						34.5	2.8	22635	
cr60-01-13db	dry	134						31.8	3.3	23950	
fr60-01-13wb	wet	79						24.5	2.4	21125	
fr60-01-13db	dry	87						23.8	2.0	21500	
cfr60-01-13wb	wet	87						23.5	2.3	21313	
cr60-01-13db	dry	86						23.5	2.0	21313	
hv-01-13WB	wet	73						68.70	3.0	31854	
hcfr-01-13WB	dry	93						68.10	3.0	31854	
v-01-16WB	wet	65				402.1	1.3	30.60	2.9	30324	342
v-01-16WB	dry	121						32.50	3.0	29200	
cr45-01-16wb	wet	57						30.40	2.6	20000	
cr45-01-16db	dry	108						28.40	2.4	24975	
cr60-01-16wb	wet	142						34.5	2.8	22635	
cr60-01-16db	dry	134						31.8	3.3	23950	
v30-03-wb	wet	99				265.5	0.9	106.4	6.3	44080	331
cr30-03-wb	wet	76						69	3.9	33637	
cfr30-03-wb	wet	99						53.8	3.7	26308	
v45-03-wb	wet	60						57	3.0	36817	
cr45-03-wb	wet	88						46.5	3.0	29586	
cfr45-03-wb	wet	70						35.5	2.6	23386	
v60-03-wb	wet	105						40.2	3.5	32113	
cr60-03-wb	wet	41						32.9	2.7	25730	
cfr60-03-wb	wet	106						29.4	2.3	21411	
vex45-03-wb	wet	61						55.3	3.6	36347	
crex45-03-wb	wet	93						46.6	3.4	29586	
cfrex45-03-wb	wet	66						35.2	2.5	21700	

Table B.2: Characteristics of Beams Studied from the Experimental Program of Kang *et al*, [13]

Test ID	Span (m)	Section		As (mm²)	ρ (%)	f'c (MPa)	ft (MPa)	E (MPa)	fyk (MPa)
		b(m)	h(m)						
H0-0.5	2.70	0.13	0.27	157.1	0.4	64.5	4.2	37700	377.0
H0-1.0				265.5	0.8	64.5	4.2	37700	407.6
H0-1.5				402.1	1.1	64.5	4.2	37700	389.1
H0-1.8				567.1	1.6	64.5	4.2	37700	410.8
H15-0.5				157.1	0.4	59.4	3.5	36200	377.0
H15-1.0				265.5	0.8	59.4	3.5	36200	407.6
H15-1.5				402.1	1.1	59.4	3.5	36200	389.1
H15-1.8				567.1	1.6	59.4	3.5	36200	410.8
H30-0.5				157.1	0.4	48.8	3.4	32800	377.0
H30-1.0				265.5	0.8	48.8	3.4	32800	407.6
H30-1.5				402.1	1.1	48.8	3.4	32800	389.1
H30-1.8				567.1	1.6	48.8	3.4	32800	410.8
N0-0.5				157.1	0.4	38.6	3.3	29200	377.0
N0-1.0				265.5	0.8	38.6	3.3	29200	407.6
N0-1.5				402.1	1.1	38.6	3.3	29200	389.1
N0-1.8				567.1	1.6	38.6	3.3	29200	410.8
N15-0.5				157.1	0.4	32.7	3	29200	377.0
N15-1.0				265.5	0.8	32.7	3	29200	407.6
N15-1.5				402.1	1.1	32.7	3	29200	389.1
N15-1.8				567.1	1.6	32.7	3	29200	410.8
N30-0.5				157.1	0.4	31.7	2.7	26500	377.0
N30-1.0				265.5	0.8	31.7	2.7	26500	407.6
N30-1.5				402.1	1.1	31.7	2.7	26500	389.1
N30-1.8				567.1	1.6	31.7	2.7	26500	410.8
N50-0.5				157.1	0.4	29	2.7	25300	377.0
N50-1.0				265.5	0.8	29	2.7	25300	407.6
N50-1.5				402.1	1.1	29	2.7	25300	389.1
N50-1.8				567.1	1.6	29	2.7	25300	410.8

Table B.3: Characteristics of Beams Studied from Ignjatovic *et al*, [12]

Test ID	Age (day)	Span (m)	Section		As (mm²)	ρ (%)	f'c (MPa)	ft (MPa)	E (MPa)	fyk (MPa)
			b (m)	h (m)						
NAC-1	29	3.0	0.20	0.30	150.8	0.3	43.7	3.1	26600	555
RAC50-1	33				150.8	0.3	44.2	2.7	26200	
RAC100-1	28				150.8	0.3	42.5	3.2	25400	
NAC-2	30				763.4	1.3	43.7	3.1	26600	
RAC50-2	35				763.4	1.3	44.2	2.7	26200	
RAC100-2	30				763.4	1.3	42.5	3.2	25400	
NAC-3	34				1272.3	2.1	43.7	3.1	26600	
RAC50-3	37				1272.3	2.1	44.2	2.7	26200	
RAC100-3	34				1272.3	2.1	42.5	3.2	25400	

Table B.4: Characteristics of Beams Studied from Ajdukiewicz and Kliszczewicz [10]

Test ID	Span (m)	Section		As (mm²)		f'c (MPa)	ft (MPa)	E (MPa)	fyk (MPa)
		b (m)	h (m)						
ONNl-b1	2.40	0.20	0.30	452.4		37.7	2.9	31900	410
ORNl-b1					0.8	34.6	2.6	25900	
ORRl-b1						29.2	2.5	21000	
ONNm-b1						57.9	3.5	35600	
ORNm-b1						56.4	3.3	31800	
ORRm-b1						55.5	2.9	26200	
GNNl-b1						39.8	3.2	27300	
GRNl-b1						40.1	2.9	24300	
GRRl-b1						36.2	2.6	22600	
GNNm-b1						58.3	4.4	32500	
GRNm-b1						60.2	4.3	28500	
GRRm-b1						54.2	3.9	26100	
GNNh-b1						89.9	6.1	36200	
GRNh-b1						85.3	5.3	35300	
GRRh-b1						84.3	4.9	30400	
BNNl-b1						40.1	3.4	36200	
BRNl-b1						35.3	3.0	31700	
BRRl-b1						31.0	2.8	26000	
BNNm-b1						61.8	4.5	41900	
BRNm-b1						57.6	3.7	35900	
BRRm-b1						55.5	3.4	31300	
BNNh-b1						103.0	6.7	51900	
BRNh-b1						105.3	6.0	43500	
BRRh-b1						97.7	5.2	39300	
ONNl-b2				804.2	1.3	38.2	3.4	37300	
ORNl-b2						36.6	2.9	28100	
ORRl-b2						30.5	2.5	21500	
ONNm-b2						59.1	3.6	37400	
ORNm-b2						58.3	3.2	31800	
ORRm-b2						57.5	3	28000	
GNNl-b2						38.7	3.1	28500	
GRNl-b2						39.3	3.0	25500	
GRRl-b2						35.8	2.7	22100	
GNNm-b2						63.7	4.4	31800	
GRNm-b2						59.6	4.1	30100	
GRRm-b2						59.2	3.8	26400	
GNNh-b2						93.4	5.9	37100	
GRNh-b2						89.1	5.1	34400	
GRRh-b2						82.2	4.8	30200	
BNNl-b2						36.6	3.5	37400	
BRNl-b2						35.8	3.2	33400	
BRRl-b2						31.4	3.0	27500	
BNNm-b2						60.8	4.1	41500	
BRNm-b2						59.6	3.6	35700	
BRRm-b2						57.6	3.3	30800	
BNNh-b2						100.9	7.2	51900	
BRNh-b2						107.8	6.3	43500	
BRRh-b2						100.5	5.1	39300	

APPENDIX C. BENDING TESTS RESULTS

Table C.1: Summary of Test Results Taken from Sato *et al.* [14].

Test ID	r	f'c/ f'c_0	Mcr (kN.m)	Mcr/Mcr_0	My (kN.m)	My/My_0	Mu (kN.m)	Mu/Mu_0	Δcr (mm)	Δy (mm)	Δy /$Δy_0$	Δu (mm)	Δu / $Δu_0$
v-01-10WB	0.00	1.00	2.1	1.0	7.4	1.00	8.0	1.00	-	6.2	1.00	94.2	1.00
v-01-10WB	0.00	1.00	1.7	1.0	7.7	1.00	9.1	1.00	-	7.4	1.00	164.4	1.00
cr45-01-10wb	0.56	0.99	2.8	1.3	7.4	1.00	8.5	1.06	-	6.4	1.03	94.0	1.00
cr45-01-10db	0.56	0.87	1.7	1.0	7.1	0.92	8.9	0.98	-	7.8	1.05	106.9	0.65
cr60-01-10wb	0.56	1.13	2.7	1.3	7.7	1.04	9.3	1.16	-	6.7	1.08	98.9	1.05
cr60-01-10db	0.56	0.98	2.1	1.2	7.8	1.01	9.5	1.04	-	7.6	1.03	116.4	0.71
v-01-13WB	0.00	1.00	3.6	1.0	13.5	1.00	13.7	1.00	-	8.9	1.00	49.8	1.00
v-01-13WB	0.00	1.00	2.1	1.0	13.2	1.00	14.0	1.00	-	9.3	1.00	80.1	1.00
cr45-01-13wb	0.56	0.99	2.8	0.8	12.9	0.96	13.9	1.01	-	8.5	0.96	52.8	1.06
cr45-01-13db	0.56	0.87	1.9	0.9	13.2	1.00	14.1	1.01	-	10.1	1.09	75.8	0.95
cr60-01-13wb	0.56	1.13	2	0.6	12.5	0.93	14.1	1.03	-	9.1	1.02	72.2	1.45
cr60-01-13db	0.56	0.98	1.4	0.7	13.4	1.02	15.1	1.08	-	8.9	0.96	73.3	0.92
fr60-01-13wb	0.48	0.80	2	0.6	12.5	0.93	13.1	0.96	-	9	1.01	44.5	0.89
fr60-01-13db	0.48	0.73	1.0	0.5	11.9	0.90	13.7	0.98	-	9.4	1.01	65.2	0.81
cfr60-01-13wb	1.00	0.77	1.5	0.4	12.4	0.92	14.1	1.03	-	8.6	0.97	70.1	1.41
cr60-01-13db	1.00	0.72	1.0	0.5	12.1	0.92	13.9	0.99	-	9.2	0.99	70.1	0.88
hv-01-13WB	0.00	1.00	3.3	1.0	13.6	1.00	16.3	1.00	-	8.3	1.00	102.2	1.00
hcfr-01-13WB	1.00	0.99	2.2	0.7	12.9	0.95	16.4	1.01	-	8.5	1.02	131.2	1.28
v-01-16WB	0.00	1.00	3.4	1.0	18.9	1.00	19.4	1.00	-	10.6	1.00	34.8	1.00
v-01-16WB	0.00	1.00	1.6	1.0	19.3	1.00	19.5	1.00	-	10.7	1.00	45.2	1.00
cr45-01-16wb	0.56	0.99	3.2	0.9	18.9	1.00	19.2	0.99	-	11.2	1.06	40.4	1.16
cr45-01-16db	0.56	0.87	1.9	1.2	18.9	0.98	19.5	1.00	-	11.2	1.05	44.7	0.99
cr60-01-16wb	0.56	1.13	1.8	0.5	18.8	0.99	19.9	1.03	-	10.8	1.02	38	1.09
cr60-01-16db	0.56	0.98	1.3	0.8	19.7	1.02	21.9	1.12	-	10.8	1.01	63.7	1.41
v30-03-wb	0.00	1.00	7.2	1.0	13.2	1.00	15.6	1.00	-	8.3	1.00	84.8	1.00
cr30-03-wb	0.58	0.65	4.5	0.6	12.5	0.95	15.3	0.98	-	8.4	1.01	76.4	0.90
cfr30-03-wb	1.00	0.51	3.7	0.5	13	0.98	15.4	0.99	-	8.7	1.05	86.8	1.02
v45-03-wb	0.00	1.00	4.3	1.0	12.9	1.00	15.0	1.16	-	8.0	1.00	81.8	1.00
cr45-03-wb	0.58	0.82	3.5	0.8	13.2	1.02	14.8	0.99	-	8.4	1.05	72.0	0.88
cfr45-03-wb	1.00	0.62	2.1	0.5	12.6	0.98	13.7	0.91	-	8.7	1.09	67.1	0.82
v60-03-wb	0.00	1.00	3.3	1.0	11.9	1.00	15.8	1.00	-	8.2	1.00	101.0	1.00
cr60-03-wb	0.51	0.82	2.7	0.8	12.8	1.08	15.3	0.97	-	9.5	1.16	86.8	0.86
cfr60-03-wb	1.00	0.73	2.4	0.7	12.2	1.03	14.1	0.89	-	9.0	1.10	59.6	0.59
vex45-03-wb	0.00	1.00	4.5	1.0	13.6	1.00	15.3	1.00	-	7.3	1.00	100.5	1.00
crex45-03-wb	0.58	0.84	4.5	1.0	13.0	0.96	15.1	0.99	-	7.7	1.05	95.7	0.95
cfrex45-03-wb	1.00	0.64	3.6	0.8	11.8	0.87	13.5	0.88	-	8.0	1.10	61.4	0.61

Table C.2: Summary of Test Results Taken from Ignjatovic [12]

Test ID	r	$f'c/f'c_0$	Mcr (kN.m)	Mcr/Mcr_0	My (kN.m)	My/My_0	Mu (kN.m)	Mu/Mu_0	Δcr (mm)	Δy (mm)	$\Delta y/\Delta y_0$	Δu (mm)	$\Delta u/\Delta u_0$
NAC-1	0.00	1.00	12.5	1.0	24.4	1.0	28.4	1.0	2.2	12.5	1.00	75.4	1.00
RAC50-1	0.33	1.01	10.0	0.8	22.5	0.9	27.0	1.0	3.2	12.8	1.02	97.9	1.30
RAC100-1	0.64	0.97	10.0	0.8	23.4	1.0	26.8	0.9	3.5	14.4	1.15	92.6	1.23
NAC-2	0.00	1.00	20.0	1.0	101.3	1.0	108.6	1.0	7.5	22.2	1.00	45.8	1.00
RAC50-2	0.33	1.01	20.0	1.0	105.0	1.0	110.6	1.0	7.4	25	1.13	46.2	1.01
RAC100-2	0.64	0.97	20.0	1.0	101.0	1.0	105.4	1.0	7.2	22.9	1.03	38.9	0.85
NAC-3	0.00	1.00	30.0	1.0	-	-	137.6	1.0	8.9	-	-	28.5	1.00
RAC50-3	0.33	1.01	30.0	1.0	-	-	160.4	1.2	8.0	-	-	34.5	1.21
RAC100-3	0.64	0.97	15.0	0.5	-	-	142.6	1.0	9.0	-	-	30.4	1.07

Table C.3: Summary of Test Results Taken from Kang *et al*, [13]

Test ID	r	$f'c/f'c_0$	Mcr (kN.m)	Mcr/Mcr_0	My (kN.m)	My/My_0	Mu (kN.m)	Mu/Mu_0	Δcr (mm)	Δy (mm)	$\Delta y/\Delta y_0$	Δu (mm)	$\Delta u/\Delta u_0$
H0-0.5	0.00	1.00	7.5	1.0	11.3	1.0	17.6	1.0	3.3	9.0	1.0	72	1.00
H0-1.0	0.00	1.00	8.4	1.0	21.7	1.0	29.6	1.0	2.5	12.0	1.0	53	1.00
H0-1.5	0.00	1.00	8.8	1.0	33.2	1.0	40.2	1.0	1.7	12.0	1.0	44	1.00
H0-1.8	0.00	1.00	9.7	1.0	46.7	1.0	56.2	1.0	2.0	15.0	1.0	36	1.00
H15-0.5	0.08	0.92	5.8	0.8	13.0	1.1	18.2	1.0	1.0	12.0	1.3	60	0.83
H15-1.0	0.08	0.92	6.6	0.8	21.7	1.0	29.3	1.0	1.3	12.0	1.0	56	1.06
H15-1.5	0.08	0.92	7.9	0.9	30.2	0.9	38.6	1.0	1.8	12.0	1.0	50	1.14
H15-1.8	0.08	0.92	9.1	0.9	45.2	1.0	58.1	1.0	2.2	15.0	1.0	41	1.14
H30-0.5	0.15	0.76	5.3	0.7	11.2	1.0	16.9	1.0	1.4	9.0	1.0	61	0.85
H30-1.0	0.15	0.76	6.2	0.7	21.9	1.0	28.8	1.0	1.0	12.0	1.0	47	0.89
H30-1.5	0.15	0.76	7.0	0.8	31.1	0.9	38.4	1.0	1.5	15.0	1.3	41	0.93
H30-1.8	0.15	0.76	7.9	0.8	46.9	1.0	49.0	0.9	1.8	18.0	1.2	21	0.58
N0-0.5	0.00	1.00	8.4	1.0	11.9	1.0	15.9	1.0	2.4	7.0	1.0	70	1.00
N0-1.0	0.00	1.00	8.8	1.0	23.3	1.0	28.2	1.0	2.4	12.0	1.0	37	1.00
N0-1.5	0.00	1.00	9.7	1.0	28.4	1.0	36.9	1.0	2.3	11.0	1.0	36	1.00
N0-1.8	0.00	1.00	14.1	1.0	48.5	1.0	52.8	1.0	3.5	17.0	1.0	26	1.00
N15-0.5	0.10	0.85	6.6	0.8	10.9	0.9	14.8	0.9	1.3	7.0	1.0	31	0.44
N15-1.0	0.10	0.85	8.0	0.9	22.6	1.0	27.2	1.0	2.0	12.0	1.0	27	0.73
N15-1.5	0.10	0.85	8.7	0.9	30.6	1.1	35.8	1.0	2.1	13.0	1.2	25	0.69
N15-1.8	0.10	0.85	12.4	0.9	47.3	1.0	51.6	1.0	3.1	15.0	0.9	20	0.77
N30-0.5	0.20	0.82	5.7	0.7	12.5	1.1	14.7	0.9	1.0	9.0	1.3	32	0.46
N30-1.0	0.20	0.82	8.0	0.9	23.5	1.0	26.3	0.9	1.7	12.0	1.0	18	0.49
N30-1.5	0.20	0.82	8.4	0.9	32.4	1.1	35.3	1.0	1.6	12.0	1.1	19	0.53
N30-1.8	0.20	0.82	12.4	0.9	44.0	0.9	50.2	1.0	3.2	16.0	0.9	24	0.92
N50-0.5	0.33	0.75	6.6	0.8	11.1	0.9	13.6	0.9	1.5	8.0	1.1	17	0.24
N50-1.0	0.33	0.75	8.0	0.9	22.6	1.0	24.4	0.9	2.1	12.0	1.0	16	0.43
N50-1.5	0.33	0.75	8.8	0.9	32.3	1.1	32.8	0.9	2.1	13.0	1.2	15	0.42
N50-1.8	0.33	0.75	11.0	0.8	48.8	1.0	50.5	1.0	2.8	17.0	1.0	20	0.77

Table C.4: Summary of Test Results Taken from Ajdukiewicz and Kliszczewicz [10]

Test ID	r	$f'c/f'c_0$	Mcr (kN.m)	Mcr/Mcr_0	My (kN.m)	My/My_0	Mu (kN.m)	Mu/Mu_0	Δcr (mm)	Δy (mm)	$\Delta y/\Delta y_0$	Δu (mm)	$\Delta u/\Delta u_0$
ONNl-b1	0.00	1.00	16.0	1.0	50.4	1.0	51.6	1.0	-	-	-	-	-
ORNl-b1	0.70	0.92	16.0	1.0	46.8	0.9	51.2	1.0	-	-	-	-	-
ORRl-b1	1.00	0.77	12.0	0.8	46.0	0.9	48.4	0.9	-	-	-	-	-
ONNm-b1	0.00	1.00	16.0	1.0	52.0	1.0	64.0	1.0	-	-	-	-	-
ORNm-b1	0.70	0.97	12.0	0.8	50.4	1.0	62.4	1.0	-	-	-	-	-
ORRm-b1	1.00	0.96	8.0	0.5	49.6	1.0	62.0	1.0	-	-	-	-	-
GNNl-b1	0.00	1.00	12.0	1.0	54.0	1.0	62.4	1.0	-	-	-	-	-
GRNl-b1	0.70	1.01	12.0	1.0	54.0	1.0	65.2	1.0	-	-	-	-	-
GRRl-b1	1.00	0.91	12.0	1.0	52.4	1.0	64.8	1.0	-	-	-	-	-
GNNm-b1	0.00	1.00	16.0	1.0	52.0	1.0	56.0	1.0	-	-	-	-	-
GRNm-b1	0.70	1.03	16.0	1.0	50.8	1.0	54.4	1.0	-	-	-	-	-
GRRm-b1	1.00	0.93	12.0	0.8	48.0	0.9	53.2	1.0	-	-	-	-	-
GNNh-b1	0.00	1.00	16.0	1.0	52.0	1.0	65.6	1.0	-	-	-	-	-
GRNh-b1	0.70	1.00	16.0	1.0	52.0	1.0	63.2	1.0	-	-	-	-	-
GRRh-b1	1.00	0.94	12.0	0.8	51.2	1.0	56.8	0.9	-	-	-	-	-
BNNl-b1	0.00	1.00	16	1.0	53.6	1.0	60.4	1.0	-	-	-	-	-
BRNl-b1	0.70	0.88	16	1.0	52.8	1.0	60.0	1.0	-	-	-	-	-
BRRl-b1	1.00	0.77	12	0.8	51.6	1.0	62.8	1.0	-	-	-	-	-
BNNm-b1	0.00	1.00	16	1.0	50.8	1.0	58.4	1.0	0.4	7	1.00	58.8	1.00
BRNm-b1	0.70	0.93	16	1.0	49.6	1.0	57.2	1.0	0.3	7.6	1.09	58.6	1.00
BRRm-b1	1.00	0.90	12	0.8	49.6	1.0	56.4	1.0	0.8	8.8	1.26	54.8	0.93
BNNh-b1	0.00	1.00	24	1.0	56.4	1.0	66.0	1.0	0.5	7.9	1.00	59.7	1.00
BRNh-b1	0.70	1.02	20	0.8	56.0	1.0	66.4	1.0	0.4	9.2	1.16	58.6	0.98
BRRh-b1	1.00	0.95	16	0.7	54.4	1.0	66.0	1.0	0.7	9.9	1.25	59.6	1.00
ONNl-b2	0.00	1.00	16.0	1.0	85.6	1.0	90.8	1.0	-	-	-	-	-
ORNl-b2	0.70	0.96	12.0	0.8	85.6	1.0	94.4	1.0	-	-	-	-	-
ORRl-b2	1.00	0.80	8.0	0.5	84.0	1.0	90.4	1.0	-	-	-	-	-
ONNm-b2	0.00	1.00	12.0	1.0	85.6	1.0	93.6	1.0	-	-	-	-	-
ORNm-b2	0.70	0.99	16.0	1.3	85.6	1.0	94.8	1.0	-	-	-	-	-
ORRm-b2	1.00	0.97	8.0	0.7	85.6	1.0	99.2	1.1	-	-	-	-	-
GNNl-b2	0.00	1.00	16.0	1.0	84.0	1.0	86.8	1.0	-	-	-	-	-
GRNl-b2	0.70	1.02	12.0	0.8	80.0	1.0	93.2	1.1	-	-	-	-	-
GRRl-b2	1.00	0.93	8.0	0.5	84.0	1.0	90.4	1.0	-	-	-	-	-
GNNm-b2	0.00	1.00	16.0	1.0	86.0	1.0	95.2	1.0	-	-	-	-	-
GRNm-b2	0.70	0.94	12.0	0.8	87.2	1.0	94.8	1.0	-	-	-	-	-
GRRm-b2	1.00	0.93	12.0	0.8	84.0	1.0	100.4	1.1	-	-	-	-	-
GNNh-b2	0.00	1.00	20.0	1.0	80.0	1.0	100.0	1.0	-	-	-	-	-
GRNh-b2	0.70	0.95	16.0	0.8	77.6	1.0	96.8	1.0	-	-	-	-	-
GRRh-b2	1.00	0.88	12.0	0.6	84.0	1.1	102.0	1.0	-	-	-	-	-

REFERENCES

[1] Etxeberria M, MarÃ- AR and VÃ¡zquez E. Recycled aggregate concrete as structural material. Materials and Structures 2007; 40(5 DO - 10.1617/s11527-006-9161-5): p. 529-541 LA - English.

[2] Etxeberria M, et al. Influence of amount of recycled coarse aggregates and production process on properties of recycled aggregate concrete. Cement and Concrete Research 2007; 37(5): 735-742. https://doi.org/10.1016/j.cemconres.2007.02.002

[3] Evangelista L and de Brito J. Mechanical behaviour of concrete made with fine recycled concrete aggregates. Cement and Concrete Composites 2007; 29(5): 397-401. https://doi.org/10.1016/j.cemconcomp.2006.12.004

[4] Xiao J, Li J and Zhang C. Mechanical properties of recycled aggregate concrete under uniaxial loading. Cement and Concrete Research 2005; 35(6): 1187-1194. https://doi.org/10.1016/j.cemconres.2004.09.020

[5] Xiao JZ, Li JB and Zhang C. On relationships between the mechanical properties of recycled aggregate concrete: An overview. Materials and Structures 2006; 39(6 DO - 10.1617/s11527-006-9093-0): p. 655-664 LA - English.

[6] Wardeh G, Ghorbel E and Gomart H. Mix Design and Properties of Recycled Aggregate Concretes: Applicability of Eurocode 2. International Journal of Concrete Structures and Materials 2014: p. 1-20 LA - English.

[7] Casuccio M, *et al*. Failure mechanism of recycled aggregate concrete. Construction and Building Materials 2008; 22(7): 1500-1506. https://doi.org/10.1016/j.conbuildmat.2007.03.032

[8] de Juan MSn and GutiÃ©rrez PA. Study on the influence of attached mortar content on the properties of recycled concrete aggregate. Construction and Building Materials 2009; 23(2): 872-877. https://doi.org/10.1016/j.conbuildmat.2008.04.012

[9] Belén GF, *et al*. Stress-strain relationship in axial compression for concrete using recycled saturated coarse aggregate. Construction and Building Materials 2011; 25(5): 2335-2342. https://doi.org/10.1016/j.conbuildmat.2010.11.031

[10] Ajdukiewicz AB and Kliszczewicz AT. Comparative Tests of Beams and Columns Made of Recycled Aggregate Concrete and Natural Aggregate Concrete. Advanced Concrete Technology 2007; 5(2): 259-273. https://doi.org/10.3151/jact.5.259

[11] Fathifazl G, *et al*. Flexural Performance of Steel-Reinforced Recycled Concrete Beams. ACI Structural Journal 2009; 106(6): 858-867.

[12] Ignjatovic IS, *et al*. Flexural behavior of reinforced recycled aggregate concrete beams under short-term loading. Materials and Structures 2013; 46(6 DO - 10.1617/s11527-012-9952-9): p. 1045-1059 LA - English.

[13] Thomas HK, Kang WK, Yoon-Keun Kwak and Sung-Gul Hong. Flexural Testing of Reinforced Concrete Beams with Recycled Concrete Aggregates. ACI Structural Journal 2014; 111(3): 607-616.

[14] Sato R, *et al*. Flexural Behavior of Reinforced Recycled Concrete Beams. Journal of Advanced Concrete Technology 2007; 5(1): 43-61. https://doi.org/10.3151/jact.5.43

[15] Eurocode 2, Design of concrete structures_Part 1-1 General rules and rules for buildings 2004: Paris.

[16] Kassoul A and Bougara A. Maximum ratio of longitudinal tensile reinforcement in high strength doubly reinforced concrete beams designed according to Eurocode 8. Engineering Structures 2010; 32(10): 3206-3213. https://doi.org/10.1016/j.engstruct.2010.06.009

[17] Park R and Paulay T. Reinforced Concrete Structures, ed. J.W. Sons. 1975, 800. https://doi.org/10.1002/9780470172834

Received on 21-11-2017 Accepted on 29-01-2018 Published on 15-02-2018

DOI: http://dx.doi.org/10.15377/2409-9848.2018.05.1

© 2018 George and Elhem; Avanti Publishers.
This is an open access article licensed under the terms of the Creative Commons Attribution Non-Commercial License (http://creativecommons.org/licenses/by-nc/3.0/) which permits unrestricted, non-commercial use, distribution and reproduction in any medium, provided the work is properly cited.